

## Memory effects in friction over correlated surfaces

Anne Tanguy and Stéphane Roux

*Laboratoire de Physique et de Mécanique des Milieux Hétérogènes, URA CNRS No. 857, Ecole Supérieure de Physique et Chimie, Industrielles de Paris, 10, rue Vauquelin, 75231 Paris Cedex 05, France*

(Received 4 October 1996)

We study the effect of a long-range correlated scale-invariant random pinning force on the motion and friction properties of an elastically driven asperity in a quasistatic regime. It is shown that when the elastic coupling is weak, the macroscopic dynamic behavior of the asperity can be described as elasto-plastic with a perfectly plastic plateau. The plastic plateau corresponds to statistically stationary sliding. The macroscopic friction behavior arises from the competition between reversible and irreversible motion due to the multiplicity of equilibrium positions. This introduces a history-dependent behavior, with marked memory effects over a characteristic length scale which is computed. This well-defined length scale is compared to the usual “memory length” considered in friction experiments. We also analyze the hardening behavior and the hysteretic behavior in radial and cyclic loadings. [S1063-651X(97)02702-5]

PACS number(s): 05.40.+j, 46.30.Pa, 62.20.Fe, 68.35.Rh

### I. INTRODUCTION

In spite of the rich variety of different rheological behaviors which can be encountered in solids, the Amonton’s laws of friction have proven to describe the vast majority of dry friction mechanical behaviors. These laws state (1) the proportionality between the tangential friction force and the normal load applied to the solids by the so-called “coefficient of friction,” “static” in the case of motionless surfaces, and “dynamic” in the case of relative sliding; and (2) the independence of the coefficient of friction on the apparent contact area between surfaces.

From experimental data, such a coefficient appears, however, to be weakly dependent on the relative velocity of solids, on contact time, or even on normal load [1]. Attempting to explain these laws, which have been observed experimentally since the time of Leonardo da Vinci, Coulomb [2] emphasized the role played by interactions between asperities at the surface of solids. Since then, these interactions have been investigated in a systematic manner, in static as well as in dynamical regimes [3,4].

Tabor gave a justification for these two laws of friction, using the fact that the real contact area is very small and thus involved such large stresses that a significant plastification occurs. Combining yield stress and shear strength, Tabor proposed the “junction growth model.” This theory led to a link between static and dynamic friction, through the evolution of the contact area, due to plastic deformation of asperities. Such a model allowed one to interpret successfully features such as the existence of a “memory length,” or “precursory stable sliding,” or “critical slip distance” observed experimentally and often presented — although their origins are generally diverse — as the “average distance needed to break a contact” [4–6]. In these cases, the saturation of the interaction force versus the relative displacement of solids results from the limitation of the total area of plastic contacts [4,7].

However, such a model seems to be inadequate for understanding the following phenomena.

(i) Possible hysteresis in friction force remaining in the

domain of “elastic” loading as could be observed in atomic force microscopy (AFM) [8].

(ii) What happens for cases where the microscopic contact behavior is elastic rather than plastic, going beyond the roughness model of Greenwood and Williamson [9]. This occurs for materials such as polymers — where the ratio of yield stress over elastic moduli (typically 1/10) is much higher than in metals (of order 1/100) — when the surface roughness is low (so that the real area of contact is large and hence the contact stresses are low). It is also well established that for such elastic contacts, the coefficient of friction depends on the normal load (in contrast to the perfectly plastic regime) and on the surface roughness, so that no general “universal” behavior can be found.

(iii) What happens when the interfacial junction stress is independent of the real contact area as in the case of boundary lubricated surfaces.

In the present theoretical study, we focus on the elastic regime, and we restrict our attention to a fixed normal load. We propose to retrieve the apparent plasticity of macroscopic behavior of solids in contact through a purely elastic model, where contact roughness exhibits long-range correlations. We consider the apparently simple case of one single asperity elastically coupled to the center of mass of a slider and constrained to move quasistatically on a rigid rough surface. In accord with microscopic models for dry friction frequently considered in the literature [10–15], energy dissipated by friction results entirely from a hysteretic process due to nonlinearity of the pinning force representing surface roughness and involving asperities of the interface between blocks. Such models are already used as models for atomic force microscopy, where the asperity is now the probing tip, and the elastic coupling accounts for the cantilever beam supporting the tip [16–18].

We describe the interaction of the asperity with the underlying surface through a time-independent scale-invariant random force with long-range correlations, for example, of self-affine statistics. Such a force accounts for characteristics of surfaces frequently encountered in nature [19]. Balancing the effect of the height correlations with the elastic coupling

gives rise to a well-defined length scale  $\xi$  which sets the amplitude of the hardening displacement. When the elastic coupling is soft, the multiplicity of equilibrium positions gives rise to a natural decomposition of the displacement of the center of mass in a reversible (elastic) part and an unrecoverable (plastic) one. This partition allows the slider to be described in the continuum limit by a simple plastic behavior, where dissipation is solely due to the irreversible part of the displacement. Hardening appears naturally in the problem through the uneven distribution of rest position of the asperity. The length scale  $\xi$  can also be seen as the displacement over which memory of the initial position is lost, and below which information on the statistics of the roughness of the surface is preserved. For such a scale-invariant force profile, the statistical distribution of jumps is analogous to that of shadows over a self-affine profile [20], and hence it is power law distributed up to  $\xi$ . The exponent appearing in the power-law is directly related to the roughness exponent of the force distribution.

Hysteretic motion of the asperity and energy dissipation are studied for cyclic as well as radial displacements imposed on the center of mass of the slider. The real asperity amplitude is shown to vary as a nontrivial power law of the center of mass amplitude.

## II. THE MODEL

We consider a single asperity with a single degree of freedom, its position  $x$ . This asperity is elastically connected to the center of mass  $\rho$  of the slider with an equivalent spring constant  $K$ , and interacts with a random pinning force field  $F(x)$  which represents the corrugation of the facing (fixed) solid. Due to the pinning force acting on the contact, the slider undergoes elastic deformation characterized by the elastic displacement of the asperity

$$u = \rho - x. \quad (1)$$

For a quasistatic motion of the center of mass of the slider, the elastic displacement self-adjusts in such a way as to equilibrate the total force acting instantaneously on the asperity, so that the position  $x$  fulfills

$$F(x) + K[x(t) - \rho(t)] = 0. \quad (2)$$

For any prescribed  $F(x)$  function, the above equation has generically an odd number  $2n + 1$  of roots, corresponding to equilibrium positions. Only  $n + 1$  of these are stable. The stability criterion reads

$$dF(x)/dx + K > 0. \quad (3)$$

Figure 1 shows a graphical construction of the stable and unstable  $x$  position for a given  $\rho$ .

Starting from a stable position  $x$ , for a prescribed  $\rho$ , one can then simply follow the evolution of  $x(t)$  when  $\rho(t)$  evolves in time. Such an evolution is governed by the ‘‘delay rule’’: whenever possible  $x(t)$  evolves continuously up to the nearest metastable equilibrium position. Without thermal activation, the only ambiguity arises when the asperity reaches the end of a stable region due to nonlinearity of the pinning force. This ambiguity should be lifted by prescribing the dy-

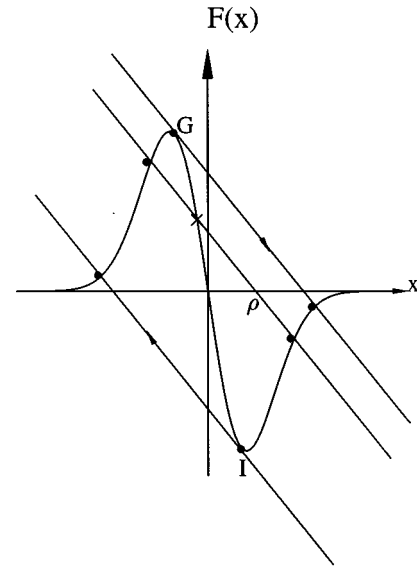


FIG. 1. Construction of the stable (symbol ●) and unstable (symbol ×) positions for a prescribed slider position  $\rho$ . The full curve is the random force function  $F(x)$ , and the dotted line has a slope  $-K$ .  $G$  and  $I$  are spinodal limits.

namical equation of motion of the asperity. In particular, one should specify an inertia and a viscous damping term taking into account to first order in velocity the various origins for dissipation. We can, however, circumvent the introduction of such additional parameters if we assume that (i) the damping term is overcritical [large enough to give rise to a monotonous exponential convergence to a stable rest position, with no oscillations in  $x(t)$ ] and (ii) the external forcing is quasistatic, so that  $\rho(t)$  does not vary significantly over the relaxation time of the asperity. In this case, we can neglect the complete time integration of the motion  $x(t)$ , and assume that the asperity simply jumps to the first stable equilibrium position for a given  $\rho(t)$ . In each jump, the damped behavior of the asperity leads to a discontinuity in the total potential energy, which corresponds to the dissipated energy, and gives rise to irreversible behavior. The dissipated energy can be seen as the work of an effective friction force, and it can easily be computed as the area between the function  $F(x)$  and a straight line of slope  $-K$  which describes the elastic coupling of the asperity. From the definition of the energy dissipation, we have

$$E_{\text{diss}} = \int_{x_0}^{x_0 + \delta} F(x_0) + Kx_0 - Kx' - F(x') dx'. \quad (4)$$

Figure 2 shows the path followed by  $x$  as  $\rho$  increases from  $\rho_0$  to  $\rho_1$  and decreases back to its initial value. The shaded area in the figure corresponds to the energy dissipated in the cycle. Under those hypotheses, the evolution of  $x(t)$  can be seen as a simple geometrical problem.

The focus of this work is to consider long-range correlated random force profile  $F(x)$ , and to analyze the statistical features of the asperity motion. In order not to introduce an intrinsic length scale yet in the model, we consider here the situation where  $F(x)$  is a self-affine function (see, e.g., Ref. [21] for an introduction), i.e., statistically invariant under the

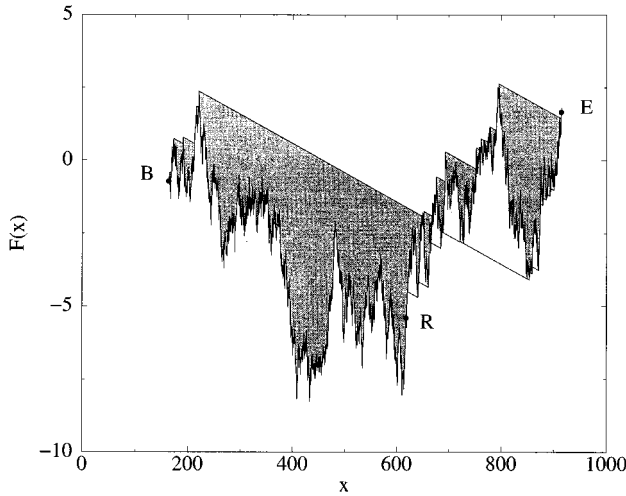


FIG. 2. Evolution of the asperity position denoted by  $x$  on the surface of the track during one cycle as  $\rho$  increases from  $\rho_0$  to  $\rho_1$  and decreases back to its original position.  $B$  points out the beginning of the motion position,  $E$  designates the position for  $\rho = \rho_1$ , and  $R$  is the position of the asperity when  $\rho$  is returning to  $\rho_0$ . The straight lines represent discontinuities in the motion of the asperity. Note that the asperity does not come back to its original position after the first cycle. The shaded area corresponds to the energy dissipated in the jumps, which can be defined as the work of the effective friction force. The lighter part of this area is due to the return path.

transformation  $x \rightarrow \lambda x$ ,  $F \rightarrow \lambda^\zeta F$ , where  $\zeta$  is a characteristic roughness exponent generally in the range  $0 < \zeta < 1$ . An easy way to construct such a function is through the inverse Fourier transform of a random phase function with an algebraic power spectrum. Namely, in the numerical simulations shown below,  $F(x)$  is computed from

$$F(x) = \sum_k A(k) k^{-1/2-\zeta} e^{-ikx}, \quad (5)$$

where  $A(k)$  is a complex randomly distributed Gaussian variable [with usual conjugation property  $\bar{A}(k) = A(-k)$  so that  $F$  is real], whose real and imaginary parts are centered on 0, and have a unit variance.

The scaling invariance of  $F(x)$  imposes that the force difference between two points at a distance  $\Delta x$  has the following scaling behavior:

$$\langle [F(x + \Delta x) - F(x)]^2 \rangle = C^2 \Delta x^{2\zeta}, \quad (6)$$

where  $C$  is a constant which gives the amplitude of the force fluctuation over a unit distance.

From the geometrical construction of the  $x$  evolution, we note an interesting correspondence with a shadowing problem. Let us consider the height  $h(x)$  of a rough surface given by  $h(x) = F(x)$ , and imagine that light is shed onto the surface from a fixed incidence angle  $\theta$  such that  $\tan(\theta) = K$ . If one is interested in  $x$  positions for increasing  $\rho$ , the topography left of the initial starting point should not be considered. Then the stable regions accessible for the asperity are exactly the lit regions of the surface. Conversely, all shadow regions cannot be reached.

The particular problem of the shadow statistics over a self-affine surface has been considered by Hansen *et al.* [20]. We simply recall here the main features uncovered in this analysis. First, there exists a characteristic length scale  $\xi$  giving the maximum extent of the shadow regions. This length scale can be obtained by matching the height difference of the rough profile and that of the incident light rays. Thus  $C\xi^\zeta = K\xi$  or

$$\xi = (C/K)^{1/(1-\zeta)}. \quad (7)$$

Second, the statistical distribution  $p(\delta)$  of the shadow length  $\delta$  can be expressed as

$$p(\delta) = 1/(\xi\delta) \phi(\delta/\xi), \quad (8)$$

where the scaling function  $\phi$  fulfills  $\phi(x) \propto x^{-\zeta}$  for  $x \ll 1$  and  $\phi$  decays to zero faster than any power law for  $x \gg 1$ . Thus the number of small jumps of size  $\delta \ll \xi$  scales as  $\delta^{-1-\zeta}$ .

In the following we will use these properties in the analysis of the motion of the asperity first under a monotonic displacement of the slider, and second in a cyclic evolution.

### III. SLIP STATISTICS

Let us consider such a steady increase of  $\rho$  and study the distribution of dissipated energy  $E_{\text{diss}}$  in jumps of size  $\delta$ . The self-affinity of  $F$  imposes that  $E_{\text{diss}}$  scales as the jump size  $\delta$ , times the force fluctuation over  $\delta$ , i.e.,

$$E_{\text{diss}} \propto \delta^{1+\zeta}. \quad (9)$$

Figure 3 shows the average value of  $E_{\text{diss}}$  for a fixed  $\delta$ , obtained for different coupling constants  $K$  ranging from 0 to 0.1, and for different roughness exponents. (Note that for this particular case, a vanishing spring constant is acceptable provided  $x$  is constrained to lie below the absolute maximum of  $F$ .) We do observe the expected power-law dependence (shown as a dotted line on the graph). From the above mentioned distribution of  $\delta$  we can deduce easily the statistical distribution of energy dissipated  $E_{\text{diss}} = E$  as

$$p(E) = 1/(K\xi^3) \psi(E/K\xi^2), \quad (10)$$

where  $\psi$  vanishes for arguments larger than 1, and behaves as a power law for small energies,  $\psi(x) \propto x^{-(1+2\zeta)/(1+\zeta)}$ , as can be shown in Fig. 4 for various stiffnesses  $K$  and various roughness exponents.

Without overemphasizing a rather loose analogy, the power-law distribution of such slips may be compared with the statistical distribution of earthquake magnitudes, which is known to obey the famous ‘‘Gutenberg-Richter law,’’ i.e., a power-law distribution  $p(E) \propto E^{-1-b}$ . In this analogy the standard  $b$  exponent amounts to  $b = \zeta/(1+\zeta)$ . Note, however, that in our model there exists an upper cutoff in the statistical distribution of energy dissipated in a slip, the existence of which is controversial in the seismology literature.

### IV. TRANSIENTS IN RADIAL LOADING

In this section we wish to analyze the memory effects, which are associated with the progressive change in the distribution of  $x$  position as the slider is moved monotonously

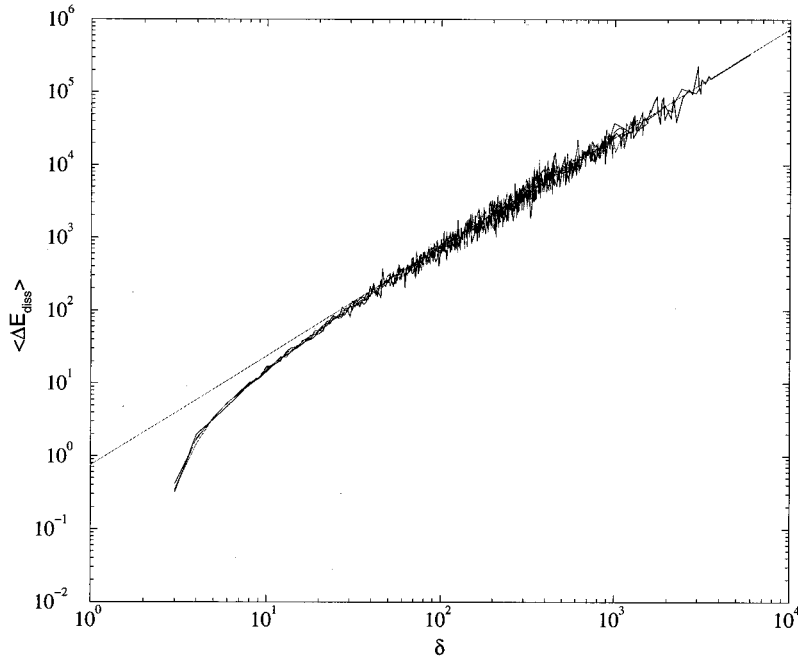


FIG. 3. Average energy dissipated in jumps of size  $\delta$ . Different elastic couplings  $K$  ranging from 0 to 0.1 are considered. The data have been averaged over 100 profiles of size  $L=16\,384$  and of roughness exponent  $\zeta=0.5$ .

from a random initial position. We term “radial loading” a monotonous increase of  $\rho$ .

When the slider is put in contact with the solid substrate, the asperity can assume any position. Therefore the average force exerted on the slider is zero, since  $\langle F \rangle = 0$ . However, as soon as the slider is moved by a distance  $\delta$ , the distribution of  $x$  position is no longer uniform. Obviously  $x$  should be stable, but more importantly, it should be accessible (i.e., not shadowed from the topography in the range  $x_0$  to  $x$ ). We have studied the average force  $\langle F \rangle$  as a function of the imposed displacement of the slider  $\rho$ . We introduce reduced variables for the displacement and the force using the characteristic scales  $\xi$  and  $K\xi \propto K^{-\zeta/(1-\zeta)}$ , respectively,  $r = \rho/\xi$  and  $f = \langle F \rangle / (K\xi)$ . Figure 5 shows a plot of  $f$  versus  $r$  as

obtained for different elastic couplings. We do observe in this plot a nice data collapse onto a master curve. For large displacements, the pinning force reaches a saturation plateau which is independent of the position. This “perfectly plastic” behavior can easily be understood as a state where the slider has lost the memory of its initial position. Whatever the way the system has been prepared, once  $\rho$  has been monotonically increased by a distance equal to the largest jump size, the statistical properties of the  $x(\rho)$  position are uniquely defined as the *minimum* stable  $x$  position among all the possible equilibrium positions for a prescribed  $\rho$ . The crossover scale is naturally  $r=1$  or  $\rho=\xi$ . For smaller slider displacements  $\rho$ , the pinning force increases with  $\rho$ . In Fig. 5 the reduced force is seen to increase linearly with  $r$ . The

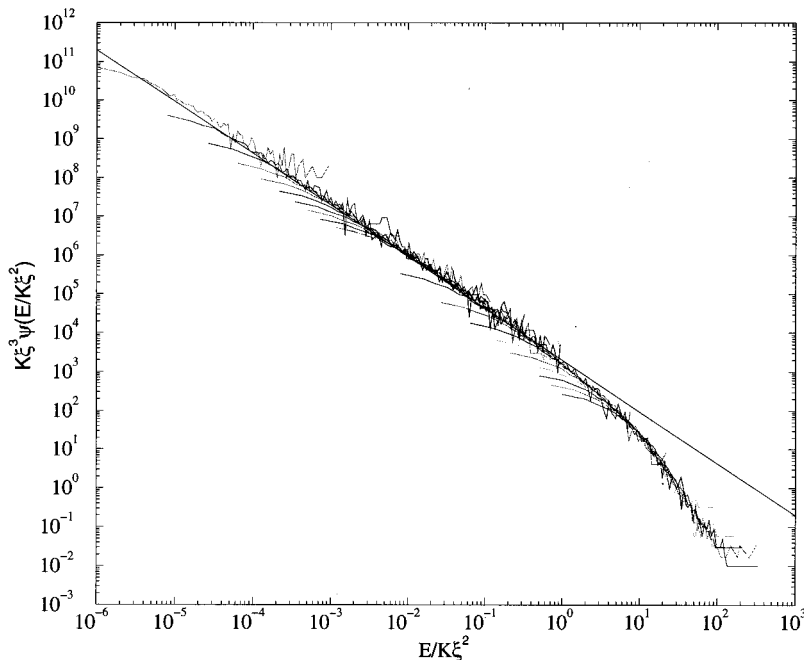


FIG. 4. Statistical distribution of the scaling function  $\Psi$  as a function of the renormalized energy  $E_{\text{diss}}/K\xi^2$ . Different elastic couplings  $K$  ranging from 0 to 0.1 are considered. The data have been averaged over 100 profiles of size  $L=16\,384$  and of roughness exponent  $\zeta=0.5$ .

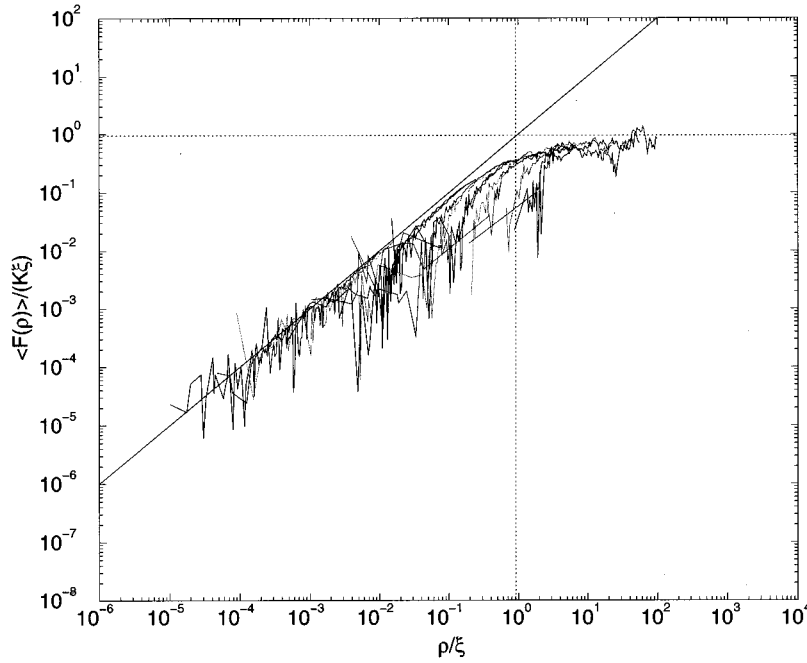


FIG. 5. Average reduced pinning force  $\langle F \rangle / K\xi$  as a function of the reduced slider displacement  $\rho/\xi$ . The average is taken over 100 profiles.

latter linear variation can be justified by considering small  $\rho$  displacements so that at most one jump occurs. Two cases are to be considered. First, the initial  $x$  position can be such that a jump occurs when  $\rho$  increases. In such a jump, the pinning force decreases by a fixed amount independent of  $r$ . The jump probability, on the contrary, depends on  $r$ , and for small distances, it grows in proportion to  $r$ . Thus the mean contribution of jumps is a net decrease of the pinning force proportional to  $r$ . Second, if no jump occurs, the pinning force increases linearly with  $r$  with a slope equal to the mean force gradient estimated on stable regions ( $dF/dx > -K$ ). The total expectation value of the pinning force change is thus linear, and has to be a net increase, consistently with the numerical results. The second contribution being the dominant one, it is natural to term this first loading phase “elastic,” since *most* of the force increase is recoverable. We will see in fact in the next section that the unrecoverable part of the displacement is not zero but is much smaller than the elastic one.

As a final remark in this section, we would like to emphasize that the difference between the pinning force and the friction force is only superficial. Whereas the former is defined as the average force  $F(x)$  acting on the asperity, the latter is defined through the averaged dissipated energy per unit distance traveled by the slider. However, integrating the equations of motion, it can easily be seen that the difference between the two forces is only the difference in potential energy between the beginning and the end of the motion.

## V. CYCLIC BEHAVIOR

We now consider friction hysteric behavior when a cyclic motion is imposed on the slider. We first notice that starting from any initial state, after one period, the asperity reaches a cyclic motion.

The imposed motion of the slider is a cycle in the range  $\rho_0$  to  $\rho_1 = \rho_0 + A$ . We are first interested in the amplitude of the limit cycle of the asperity which explores the interval

from  $x_0$  to  $x_1 = x_0 + B$ . Because of the pinning force, the asperity does not precisely follow the slider. The amplitude  $B$  is such that the typical force difference over  $B$ , i.e.,  $CB^\zeta$  matches the change in the elastic force exerted by the slider on the asperity, i.e.,  $K(A - B)$ . This provides the required asperity cycle amplitude

$$A = B + \left(\frac{C}{K}\right) B^\zeta = B + \xi \left(\frac{B}{\xi}\right)^\zeta. \quad (11)$$

As in the preceding section we introduce reduced amplitudes  $a = A/\xi$  and  $b = B/\xi$ , so that we have

$$a = b + b^\zeta. \quad (12)$$

Thus two regimes have to be distinguished: for low  $a \ll 1$  amplitudes, we have  $b \approx a^{1/\zeta} - a^{(1-\zeta)/\zeta^2} - \dots$ , whereas for large amplitude  $a \gg 1$ , we have  $b \approx a - a^\zeta - \dots$ .

Figure 6 shows a plot of  $b$  versus  $a$  displaying the two expected behaviors. From the above argument, to derive the asperity cycle amplitude, we again note that  $\xi$  gives the memory length scale over which the asperity is slaved on the average to the slider motion. Below this scale the self-affine nature of the force profile gives rise to a nontrivial variation of  $b$  versus  $a$ . For low amplitude of the slider motion, the asperity is “pinned” in a local region and does not explore much of the facing surface.

Once the amplitude of the asperity cycle has been determined, we can have access to the energy dissipated in a cycle. This energy  $E_{\text{diss}}$  is again turned into a reduced variable, by scaling it with  $K\xi^2$ ,  $\epsilon = E_{\text{diss}}/(K\xi^2)$ . For small amplitude,  $a \ll 1$ , the largest jump encountered in the asperity motion is proportional to the asperity amplitude, so that the energy dissipation is simply proportional to  $b^{1+\zeta}$  as a result of Eq. (9). Thus  $\epsilon \propto a^{(1+\zeta)/\zeta}$ . When the amplitude gets larger,  $a \gg 1$ , then the energy dissipated in one cycle is proportional to the number of largest jumps  $B/\xi$  times the energy dissipated in such a jump, hence  $\epsilon \propto a$ .

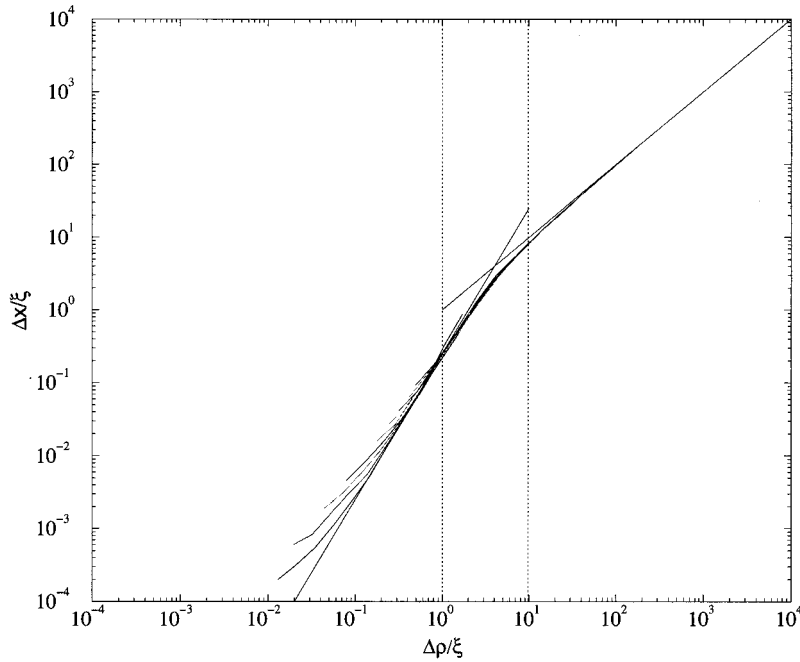


FIG. 6. Reduced asperity displacement amplitude  $\Delta x/\xi$  versus reduced slider amplitude  $\Delta\rho/\xi$ . Average considered over 100 samples and ten different elastic couplings  $K$  from 0 to 0.1.

Figure 7 shows the reduced energy dissipation  $\epsilon$  versus the reduced slider amplitude  $a$ . We again observe a good data collapse of the mean energy dissipated for various elastic couplings, and the two above described regimes.

In the particular case of uncorrelated surfaces, the behavior of the pinning force exhibits only a perfect plastic plateau. For Greenwood-Williamson surfaces [9], for example, where bumps of radius of curvature  $R$  are exponentially distributed in height without correlations, the regime at small displacement  $\Delta\rho$  is dominated by the correlations induced by the nonzero radius of curvature  $R$  and the continuity condition for the surface. At larger displacements, the dissipative energy is dominated by the energy dissipated over large jumps of size  $\xi$  scaling in  $1/K$ .

## VI. PLASTICITY

The plasticity appears here as a macroscopic irreversibility of the dynamical behavior of the asperity.

From the previously reported analysis, we see that the observed mean behavior of the two solids in contact can be accurately described as elasto-plastic with a perfect plasticity plateau. This correspondence is actually deeper than just an image deduced from the shape of the force versus displacement plots.

One basic step in the description of an elasto-plastic constitutive law is the partition of the strain into an elastic recoverable part and an irreversible plastic strain. In our case, such a partition has a clear origin: the plastic displacement corresponds to the jumps. It is the only component which

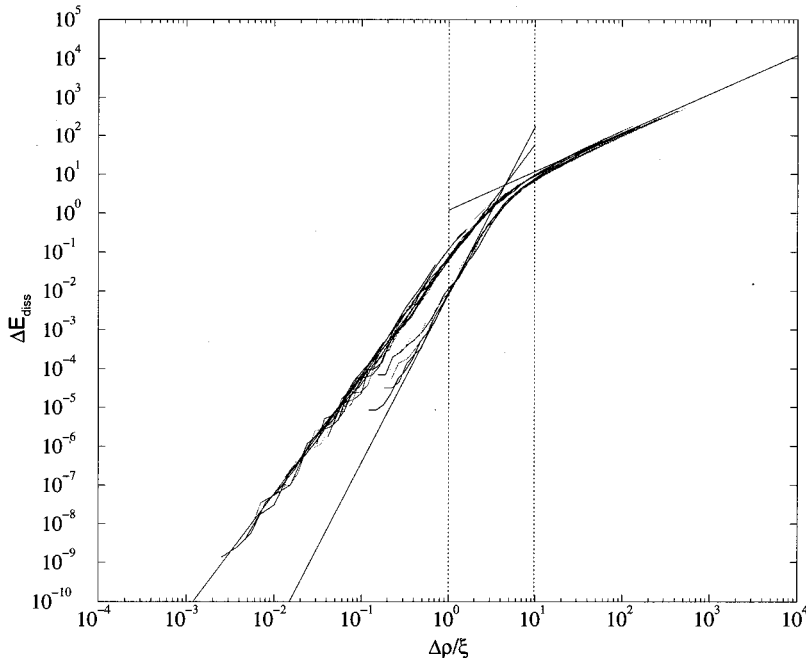


FIG. 7. Reduced energy dissipation  $E_{\text{diss}}/(K\xi^2)$  versus reduced slider amplitude  $\Delta\rho/\xi$ . Average considered over 100 samples of size  $L=16\,384$ , of various roughness exponents  $\zeta=0.3$ ,  $\zeta=0.5$  and for different elastic couplings  $K$  from 0 to 1.

induces energy dissipation. The total displacement of the asperity also contains an additional component which corresponds to the motion along stable regions of the force profile. This part is reversible and contributes solely to the potential energy of the system. The previous study showed that, for small  $\rho$  displacements ( $\rho \ll \xi$ ), the elastic contribution in  $\rho$  to the average pinning force is dominant. This is due to the fact that the  $x$  behavior is dominated by the increasing delay distance between asperity and slider center of mass  $x \approx \rho^{1/\xi} \ll \rho$  due to the roughness of the surface, so that finally

$$F_p(\rho) \approx K\rho. \quad (13)$$

Such an “elastic regime” goes together with a gradual hardening — the jumps remaining an essential component of the motion on the random surfaces. However, for large displacements, the contribution due to the jump dominates. The asperity follows on average the motion of the center of mass of the slider, so that a stationary regime is reached, and the maximum jump size saturates. The average pinning force is constant,

$$F_p(\rho) \approx K\xi. \quad (14)$$

This regime is assimilated to a “sliding” regime.

The “elastic” behavior of the asperity is then due to pinning on the random force. As the driving force is increased, pinning vanishes — gradually in the case of long-range finite correlations of the pinning force or suddenly in the case of uncorrelated pinning force — giving rise at the end to a stationary “sliding” behavior.

The key feature which introduces some variance as compared to the standard plasticity description is the accompanying statistical feature of the jump distribution, with power-law distribution up to a limiting intrinsic scale which scales with the stiffness of the system.

Note, however, that such statistical reasoning assumes that the observed range of scaling is *large* compared to the lower cutoff of the random force. Inversely, the “elastic domain” is observable *below* the characteristic length  $\xi$ .

We conclude, emphasizing that the plasticity results entirely from the nonlinear coupling between volume elastic properties of the slider and surface roughness properties of the track. It thus does not require any irreversible process in the bulk of the slider.

## VII. DISCUSSION

The existence of an internal length over which the friction properties evolve has been recognized for some time, and thus different rheological models have been proposed to account for it [22,23], through the introduction of internal variables. Using simple description of the topography as consisting in isolated bumps, this distance is usually interpreted in terms of “distance between bumps,” or “distance needed to break a contact,” which remains to be more firmly justified.

In the case of the Ruina model [23], the constitutive law of internal variables depends on time and describes the phenomenological evolution of the properties of the surfaces of solids in contact. In our case, the hardening — appearing through the dynamical behavior of the asperities at surfaces — does not need any modification of the surfaces in contact,

or intrinsic time evolution of the mechanical properties, but appears as an unavoidable consequence of the instability model of Ref. [12]. Of course, such a model does not take into account evolution of the static friction coefficient versus contact time. The study of this dependence would require at least introduction of thermal activation. However, separation between static and dynamic mechanisms is not in contradiction with the marked difference observed in temperature-dependent experiments [24].

Restricting to the present study, note that the stick behavior is characterized essentially by a strong slowing down due to roughness and by an irreversible behavior progressively overwhelming the elastic component of the displacement. Real stick could appear only in the case of uncorrelated surfaces, where the asperity motion is completely decorrelated from the center of mass motion, over length scales comparable to the cutoff. In such cases, the scaling of the characteristic length  $\xi$  in  $1/K$  does not depend on the probability law.

The characteristic length  $\xi$  is shown to depend on the elastic constant  $K$  of the slider, on the roughness exponent  $\zeta$ , and on the amplitude of the roughness of the track (at fixed length scale). Respective contributions of slider and track properties are asymmetric. More realistic description of friction must take into account the correlations between multiple asperities of the slider as well as elastic properties of the track considered, for instance, as infinitely rigid. Such a model could, however, be of interest for interpreting AFM measurements [8].

Nevertheless, the restriction to a one-dimensional variable  $x$  does not prevent any application to collective interactions. Some systems are well described, in the limit of weak distortions, by a comparable one-variable equation, where  $x$  denotes the average position of the system and where the pinning force  $F(x)$  is replaced by an effective force obtained by minimizing the pinning force over the other variables. It is, for example, the case of a fluid interface in contact with a heterogeneous solid surface [25]. In this case, the perturbation induced by a local force applied on the contact line heals on a distance of the order of the capillary length taken as the size of the system. The pinning force is due to the interaction of the contact line with defects on the solid surface. The traction results from the combined effects of gravity and of surface tension on the interface. The motion is imposed on the solid dipped into the liquid bath. Such a system exhibits hysteresis in the average position of the contact line, thus in the contact angle  $\theta$ .

In the quite different domain of seismic faulting, Scholz [26] proposed considering analogous distance for interpreting the depth dependence of the “critical slip distance,” a crucial feature for earthquake modeling. However, the argument proposed in this last reference is based on the elastic mating of the two facing surfaces which is shown to occur above a pressure-dependent wavelength. The identification between  $\xi$  and the maximum wavelength of the elastically deformed fault is not firmly established but rather argued for, using criteria such as “complete renewal of contact population.” Although the conclusions may be qualitatively compared to that of our model (the critical slip distance results from the competition of the surface topography and the elastic coupling and is not intrinsic to the material or surface

topography), the approach to the problem is quite different and any further comparison appears difficult.

### VIII. CONCLUSION

The friction law involving asperity behavior appears to be an idealization of phenomena occurring close to the interface, and the bulk properties of the solid can never be forgotten. We have presented a model where the effective friction law results from the competition of the random interaction potential on the surface and the elastic properties of the solid (here reduced to the elastic coupling between the asperity and the center of mass of the solid).

In the apparently simple case of a single asperity driven quasistatically on a rough track, we have shown the existence of a well-defined scale  $\xi$  which separates two distinct regimes. This length scale emerges from the competition between the elastic coupling and the rapidly varying random force field affecting the asperity. It depends on the stiffness of the slider as well as on the roughness exponent  $\zeta$  characterizing the long-range correlations of the roughness of the rigid track. It is to be noted that the underlying force field was chosen here as scale invariant so that no intrinsic length scale was initially included in the interacting potential, in contrast to previous models.

Although our model is purely elastic, the global behavior is plastic, with a hardening taking place statistically over a

scale  $\xi$ . After the slider has traveled a distance of order  $\xi$ , the friction force reaches a nonzero average, although a spatial average of the random force  $F$  is null. This difference comes from the bias introduced by the uneven distribution of the position of the asperity.

The persistence of a hysteretic behavior even in the ‘‘elastic’’ part of the force-displacement curve comes from the randomness of the pinning force. The long-range correlations of this force allow the slider to advance elastically. In the case of an uncorrelated surface, such an elastic regime does not exist.

Memory effects are analyzed for cyclic loadings, and it is shown that the real amplitude of motion of the asperity is much smaller than that imposed on the center of mass of the slider, for amplitude smaller than the characteristic scale  $\xi$ . Below this scale, the behavior of the system is seen to preserve statistical information on the roughness of the track and to be affected by its history.

### ACKNOWLEDGMENTS

It is a pleasure to acknowledge enlightening discussions with Ch. Fretigny, H.J. Herrmann, F. Plouraboué, and D. Vandembroucq. This work is partly supported by the Groupement de Recherche ‘‘Physique des Milieux Hétérogènes Complexes’’ of the CNRS.

- 
- [1] F. Bowden and D. Tabor, *Friction and Lubrication of Solids* (Clarendon Press, Oxford, 1950).
  - [2] C.A. Coulomb, *Theorie des Machines simples* (Memoire de Mathematique et de Physique de l’Academie Royale, Paris, 1785), pp. 161–342.
  - [3] E. Rabinowicz, *Friction and Wear of Materials* (Wiley, New York, 1965).
  - [4] J.H. Dieterich and B.D. Kilgore, *Pure Appl. Geophys.* **143**, 283 (1994).
  - [5] F. Heslot, T. Baumberger, B. Perrin, B. Caroli, and C. Caroli, *Phys. Rev. E* **49**, 4973 (1994).
  - [6] C.H. Scholz, *The Mechanics of Earthquakes and Faulting* (Cambridge University, Cambridge, England, 1990).
  - [7] J.S. Courtney-Pratt and E. Eisner, *Proc. R. Soc. London, Ser. A* **238**, 529 (1957).
  - [8] T. Göddenhenrich, S. Müller, and C. Heiden, *Rev. Sci. Instrum.* **65**, 2870 (1994).
  - [9] J.A. Greenwood and J.P.B. Williamson, *Proc. R. Soc. London, Ser. A* **295**, 300 (1966).
  - [10] C. Caroli and P. Nozières, in *The Physics of Sliding Friction*, edited by B.N.J. Persson, Vol. 311 of NATO Advanced Study Institute Series E: Applied Sciences (Kluwer, Dordrecht, 1996).
  - [11] A. Tanguy and P. Nozières, *J. Phys. (France) I* **6**, 1251 (1996).
  - [12] G.A. Tomlinson, *Philos. Mag.* **7**, 905 (1929).
  - [13] I.L. Singer, *J. Vac. Sci. Technol. A* **12**, 2605 (1994).
  - [14] J.B. Sokolov, *Phys. Rev. B* **14**, 4281 (1990).
  - [15] H.J. Jensen, Y. Bréchet, and B. Douçot, *J. Phys. (France) I* **3**, 611 (1993).
  - [16] T. Gyalog, M. Bammerlin, R. Lüthi, E. Meyer, and H. Thomas, *Europhys. Lett.* **31**, 269 (1995).
  - [17] N. Sasaki, K. Kobayashi, and M. Tsukada, *J. Appl. Phys.* **35**, 3700 (1996).
  - [18] C.M. Mate, G.M. McClelland, R. Erlandsson, and S. Chiang, *Phys. Rev. Lett.* **59**, 1942 (1987).
  - [19] P. Meakin, *Phys. Rep.* **235**, 189 (1993).
  - [20] A. Hansen, F. Plouraboué, and S. Roux, *Fractals* **3**, 91 (1995).
  - [21] J. Feder, *Fractals* (Plenum, New York, 1988).
  - [22] J.H. Dieterich, *J. Geophys. Res.* **84**, 2161 (1979).
  - [23] A.L. Ruina, *J. Geophys. Res.* **88**, 10 359 (1983).
  - [24] T. Baumberger and P. Berthoud (private communication).
  - [25] J. Crassous and E. Charlaix, *Europhys. Lett.* **28**, 415 (1994).
  - [26] C. H. Scholz, *Nature (London)* **336**, 761 (1988).